

Ultrashort Echo Time Imaging of the Osteochondral Junction in Subjects with Knee Osteoarthritis and Age-matched Healthy Volunteers

James W MacKay¹, Josh Kaggie¹, Alexandra R Morgan², Rob Janiczek², Scott Reid³, Stephen McDonnell⁴, Wasim Khan⁴, Martin Graves¹, Fiona J Gilbert¹, and Andrew McCaskie⁴

¹Radiology, University of Cambridge, Cambridge, United Kingdom, ²Experimental Medicine Imaging, GlaxoSmithKline, Stevenage, United Kingdom, ³GE Healthcare, Little Chalfont, United Kingdom, ⁴Trauma & Orthopaedics, University of Cambridge, Cambridge, United Kingdom

Synopsis

We describe *in vivo* translation of ultrashort TE (UTE) imaging of the osteochondral junction (OCJ) at the knee in 9 subjects with osteoarthritis (OA) and 4 age-matched healthy volunteers. The OCJ plays an important role in onset and progression of OA. Our study demonstrates that UTE imaging of the OCJ is repeatable and demonstrates OCJ defects in OA subjects but not in healthy volunteers. Areas of OCJ damage commonly co-locate to other osteochondral pathology (bone marrow lesions and cartilage defects). UTE imaging of the OCJ may be a helpful tool for assessing OCJ damage in clinical studies of OA.

Introduction

Disruption of the osteochondral junction (OCJ) is thought to play an important role in the onset and progression of osteoarthritis (OA). Using conventional MR imaging, direct visualisation of the OCJ is not possible due to inherent short T1 and T2 relaxation times of the OCJ tissues. However, by achieving echo times (TEs) of < 1 ms, ultrashort echo time (UTE) MR imaging allows direct visualisation of the OCJ. The normal OCJ appears as an area of linear high signal intensity (SI) on UTE images at the bone-cartilage interface. In OA it has been shown that this area of linear high SI can become thinned or absent, compatible with histological findings of OCJ defects^{1,2}. These findings have been described in a number of cadaveric MR studies, but there are limited *in vivo* data available³⁻⁵.

The aims of this study were to compare the *in vivo* appearance of the OCJ on UTE MR imaging between subjects with knee OA and age-matched healthy volunteers, to determine the relationship between OCJ defects and other osteochondral pathology, and to assess test-retest repeatability.

Methods

We imaged 9 participants with mild-moderate knee osteoarthritis, characterised by radiographs with medial tibiofemoral compartment predominant disease and Kellgren-Lawrence grades 2-3, and 4 age-matched healthy volunteers. Participants were imaged at baseline and 1 month.

MR studies were performed on a 3T system (GE 750, GE Healthcare). The MR protocol consisted of standard clinical sequences (coronal and sagittal intermediate-weighted fat-saturated fast spin echo (FSE) sequences plus a coronal T1-weighted FSE sequence) and a sagittal dual-echo UTE gradient echo sequence acquired using a 3D cones trajectory (research prototype; repetition time 15 ms, TE 0.03/4.5 ms, flip angle 13°, field-of-view 18 x 18 cm, matrix 430 x 430, slice thickness 2 mm, number of averages 1, acquisition time ~ 7.5 minutes).

To increase conspicuity of short T2 tissues, we performed weighted digital image subtraction of the longer TE (4.5 ms) from the shorter TE images (0.03 ms)⁶. The presence or absence of characteristic linear high SI at the OCJ was scored in 12 regions for each knee, corresponding to tibiofemoral subdivisions commonly used for semi-quantitative scoring. The presence of bone marrow lesions (BML) or cartilage defects in the same regions was also recorded. Assessment was performed by a single musculoskeletal radiologist with 5 years' experience in OA research, blinded to group assignment.

We used descriptive statistics to compare the number of regions with OCJ defects in subjects with OA and healthy volunteers, and to assess the frequency with which OCJ defects co-located with BMLs or cartilage defects. Test-retest repeatability was evaluated using kappa statistics.

Results

Participant characteristics are displayed in table 1.

Six out of 9 OA participants (67%) had an OCJ defect in at least one region compared to 0 out of 4 controls (0%). The most commonly involved region was the central medial tibia (4 participants). OCJ defects commonly co-located to BMLs (7 out of 10 OCJ defects, 70%) and cartilage defects (6 out of 10 OCJ defects, 60%). Results are displayed in table 2. Sample images are displayed in figures 1 – 3.

The kappa value for test-retest repeatability of OCJ assessment using UTE was 0.83 (95% confidence interval 0.64 to 1).

Discussion

The appearances of OCJ defects in subjects with OA *in vivo* are in keeping with abnormalities predicted by cadaveric MR and histology studies^{1,3}. The biological plausibility of the findings is enhanced by the frequency of co-location of OCJ damage to other osteochondral pathology (BMLs and cartilage defects). Our findings demonstrate *in vivo* translation of UTE imaging of the OCJ, and suggest that this is a useful tool for future studies of OA onset and progression. This may include predicting response to intervention, as equine studies have demonstrated that the presence or absence of OCJ damage is an important predictor of response to treatment of cartilage defects⁷.

Our results demonstrate that UTE imaging of the OCJ is repeatable with kappa values in keeping with 'near-perfect' test-retest repeatability for qualitative assessment⁸.

Previous *in vivo* studies have not used age-matched control subjects, therefore it has been unclear whether areas of OCJ damage are related to OA or normal ageing⁴. The normal appearance of the OCJ in age-matched control subjects in this study suggests that the OCJ defects are not part of normal ageing, although at present the number of healthy volunteers imaged is small.

Conclusion

In vivo UTE MR imaging of the OCJ is repeatable and demonstrates OCJ defects in subjects with OA. OCJ defects commonly co-locate with other osteochondral pathology.

Acknowledgements

The research team acknowledge the support of the NIHR Cambridge Biomedical Research Centre.

References

- Lane LB, Bullough PG: Age-related changes in the thickness of the calcified zone and the number of tidemarks in adult human articular cartilage. *J Bone Joint Surg Br* 1980; 62:372–375.
- Li B, Marshall D, Roe M, Aspden RM: The electron microscope appearance of the subchondral bone plate in the human femoral head in osteoarthritis and osteoporosis. *J Anat* 1999; 195 (Pt 1):101–110.
- Bae WC, Dwek JR, Znamirovski R, et al.: Ultrashort Echo Time MR Imaging of Osteochondral Junction of the Knee at 3 T: Identification of Anatomic Structures Contributing to Signal Intensity. *Radiology* 2010; 254:837–845.
- Mackay JW, Low SBL, Houston GC, Toms AP: Ultrashort TE evaluation of the osteochondral junction in vivo: a feasibility study. *Br J Radiol* 2016; 89:20150493.
- Du J, Carl M, Bae WC, et al.: Dual inversion recovery ultrashort echo time (DIR-UTE) imaging and quantification of the zone of calcified cartilage (ZCC). *Osteoarthritis Cartilage* 2013; 21:77–85.
- Robson MD, Gatehouse PD, So PW, Bell JD, Bydder GM: Contrast enhancement of short T2 tissues using ultrashort TE (UTE) pulse sequences. *Clin Radiol* 2004; 59:720–726.
- Frisbie DD, Morisset S, Ho CP, Rodkey WG, Steadman JR, McIlwraith CW: Effects of Calcified Cartilage on Healing of Chondral Defects Treated With Microfracture in Horses. *Am J Sports Med* 2006; 34:1824–1831.
- Landis JR, Koch GG: The measurement of observer agreement for categorical data. *Biometrics* 1977; 33:159–174.

Figures

Table 1 – Participant characteristics

Variable	OA subjects (n = 9)	Healthy volunteers (n = 4)
Age*	52 (41 to 57)	55 (53 to 58)
Sex (M:F)	5:4	2:2
BMI*	29 (24 to 31)	28 (26 to 31)
Oxford Knee Score*	22 (12 to 35)	48 (all 48)
VAS pain*	5.4 (3.7 to 6.9)	0 (all 0)
KOOS-5*	40 (28 to 64)	100 (99 to 100)

*mean (range)

Abbreviations: BMI – body mass index, VAS – visual analogue scale, KOOS-5 – knee injury and osteoarthritis outcome score, average across 5 subscales.

Table 1 - Participant Characteristics.

Table 2 – Summary of study findings.

Group	OA (n = 9)				Healthy volunteer (n = 4)			
	MF	MT	LF	LT	MF	MT	LF	LT
Number of OCJ defects detected	2	6	1	1	0	0	0	0
BML co-location*	2 (100)	3 (50)	1 (100)	1 (100)	-	-	-	-
Partial thickness cartilage defect co-location*	0 (0)	1 (17)	1 (100)	0 (0)	-	-	-	-
Full thickness cartilage defect co-location*	2 (100)	2 (33)	0 (0)	0 (0)	-	-	-	-

*n (%)

Abbreviations: MF – medial femur, MT – medial tibia, LF – lateral femur, LT – lateral tibia, OCJ – osteochondral junction, BML – bone marrow lesion

Table 2 - Summary of study findings. For purposes of clarity, the subregions scored have been condensed into 4 larger regions. Each of these larger regions contains 3 subregions, corresponding to anterior, central and posterior divisions.

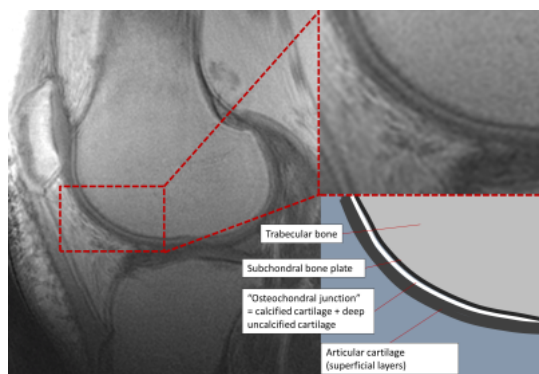


Figure 1 - Sagittal UTE image through the lateral compartment of a healthy volunteer demonstrating the normal appearance of the osteochondral junction (left panel) with enlarged view (top right) and schematic representation (bottom right).

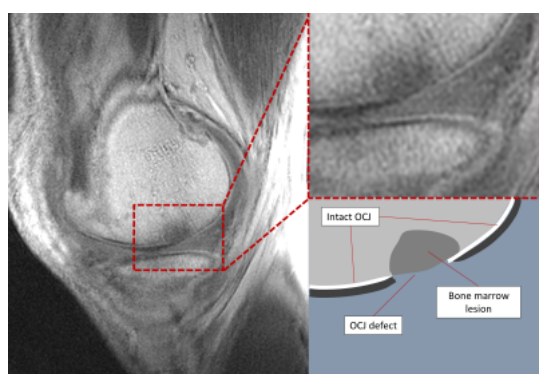


Figure 2 - Sagittal UTE image through the medial compartment of an OA subject demonstrating an OCJ defect (left), with enlarged view (top right) and schematic representation (bottom right).

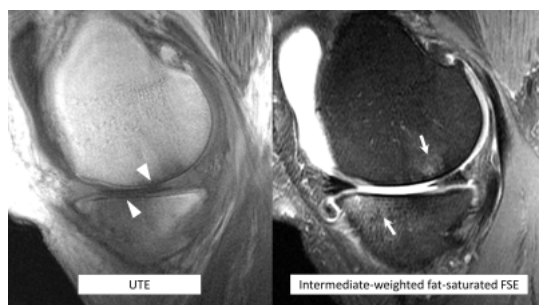


Figure 3 - Example of co-location of OCJ defects (white arrowheads) on a sagittal UTE image (left panel) to a bone marrow lesion underlying an area of full thickness cartilage loss (white arrows) on a sagittal intermediate weighted, fat-saturated image (right panel) through the medial compartment of a subject with OA.